

# Initial Eccentricity in Deformed $^{197}\text{Au}+^{197}\text{Au}$ and $^{238}\text{U}+^{238}\text{U}$ Collisions at RHIC

Peter Filip, Richard Lednicky, Hiroshi  
Masui, and Nu Xu

*This work was supported by the Director, Office of  
Science, Office of Nuclear Science of the U.S.  
Department of Energy under Contract No. DE-AC02-  
05CH11231.*

Peter Filip,\* Richard Lednicky, Hiroshi Masui, and Nu Xu  
*Institute of Physics, Slovak Academy of Sciences, Bratislava, Slovakia*  
*Joint Institute for Nuclear Research, Dubna, Russia and*  
*Lawrence Berkeley National Laboratory, Berkeley, 94705, USA*

Initial eccentricity and eccentricity fluctuations of the interaction volume created in relativistic collisions of deformed  $^{197}\text{Au}$  and  $^{238}\text{U}$  nuclei are studied using optical and Monte-Carlo (MC) Glauber simulations. It is found that the non-sphericity noticeably influences the average eccentricity in central collisions and eccentricity fluctuations are enhanced due to deformation. Quantitative results are obtained for Au+Au and U+U collisions at energy  $\sqrt{s_{NN}}=200$  GeV.  
 PACS number(s): 25.75.Ld, 21.10.Ft

## I. INTRODUCTION

Measurement of the elliptic flow [1] and higher-order azimuthal asymmetries [2] in transverse momentum distributions of particles created in relativistic nucleus-nucleus collisions at RHIC [3] provides us with the possibility to study collective properties of strongly interacting partonic matter [4]. Hydrodynamical simulations [5] of ultra-relativistic heavy ion collisions at RHIC are often used to determine quantitatively bulk properties of the expanding QCD matter created [6]. As an initial condition in hydrodynamical simulations, the asymmetrical shape (eccentricity  $\varepsilon$ ) of the interaction volume of compressed partonic matter has to be specified [7].

In collisions of spherical nuclei the geometry of the interaction volume is simply related to the impact parameter and the centrality of collisions [8]. However, in collisions of deformed nuclei the geometrical orientation of nuclei relative to each other and to the beam axis influences directly initial eccentricity  $\varepsilon$  as well as number of binary nucleon-nucleon collisions  $N_{\text{coll}}$  and number of participants  $N_{\text{part}}$  in such collisions. It is important to clarify the influence of nuclear ground-state deformation on the initial conditions in nucleus-nucleus collisions, because relativistic interactions of slightly deformed nuclei (Si, Au, Cu, In) [9] have already been studied at AGS [10], SPS [11], and RHIC [12]. Moreover, precise understanding of the initial geometry of the partonic matter created in ultra-relativistic collisions of heavy prolate nuclei is needed for a reliable interpretation of forthcoming experiments with  $^{238}\text{U}$  beams at RHIC. (Colliding heavy prolate nuclei may provide higher particle density and longer duration in certain configurations).

The relevance of slight ground-state deformation of  $^{197}\text{Au}$  nucleus in relativistic Au+Au collisions at RHIC has been risen only recently [13]. **Although electron scattering experiments [14] suggest charge distribution in  $^{197}\text{Au}$  nucleus to be spherical, non-zero quadrupole moment ( $Q=0.587 \pm 5\%$ ) is obtained for  $^{197}\text{Au}$  from recent hyperfine interaction**

**measurements [15]. Theoretical calculations [9] predict oblate deformation ( $\beta_2=-0.13$ ) for  $^{197}\text{Au}$  ground state and also giant dipole resonance measurement in  $^{197}\text{Au}(\gamma,n)$  reaction [16] suggests significant oblate  $^{197}\text{Au}$  deformation ( $|\beta_2| \approx 0.15$ ).**

In this paper we study the average eccentricity and eccentricity fluctuations of the interaction volume in collisions of deformed nuclei ( $^{197}\text{Au}$  and  $^{238}\text{U}$ ) using optical Glauber [17] and MC Glauber Model [18] simulations.

## II. GLAUBER MODEL SIMULATION FOR DEFORMED NUCLEI

The implementation of deformed nuclear shape in our Glauber model simulations has been done in the following way: Spatial distribution of nucleons has been generated according to deformed Woods-Saxon density [19]

$$\rho_w(x, y, z) = \frac{\rho_o}{1 + e^{(r-R_o(1+\beta_2 Y_{20}+\beta_4 Y_{40}))/a}} \quad (1)$$

with deformation parameters ( $\beta_2=-0.13$ ,  $\beta_4=-0.03$ ) taken from [9] for  $^{197}\text{Au}$  ( $R=6.38$  fm,  $a=0.53$ ). For U+U collisions we have used  $\beta_2 = 0.28$  in agreement with [21] and  $\beta_4 = 0.093$  was implemented according to [9]. Deformation parameter  $\beta_4$  for  $^{238}\text{U}$  nucleus ( $R=6.81$ ,  $a=0.54$ ) should be taken into account in U+U simulations since it noticeably influences the shape of the nucleon density in the core of  $^{238}\text{U}$  nucleus. Consequently, initial conditions of hydrodynamical simulations of U+U collisions depend on  $\beta_4$  parameter used. In Fig.1 we show transverse profile of participant nucleon density  $\rho_p$  obtained using optical Glauber calculation for body-body U+U collision (symmetry axes of U nuclei are orthogonal to the beam, collinear and impact  $b=0$  fm). Although total eccentricity of participants is only slightly modified assuming  $\beta_4 \neq 0$ , the eccentricity of the high-density core ( $\rho_p > \rho_{\text{cut}}$ ) is significantly dependent on  $\beta_4$  (see Fig.1b). This can have substantial influence on the elliptic flow strength obtained in hydrodynamical simulations [20].

In our calculations, nuclei have been rotated randomly to simulate unpolarized nucleon-nucleon collisions, which gives probability distribution  $P(\theta) = \sin(\theta)/2$  for polar angles  $\theta_1, \theta_2$  and random distribution of azimuthal angles

---

\*Peter.Filip@savba.sk

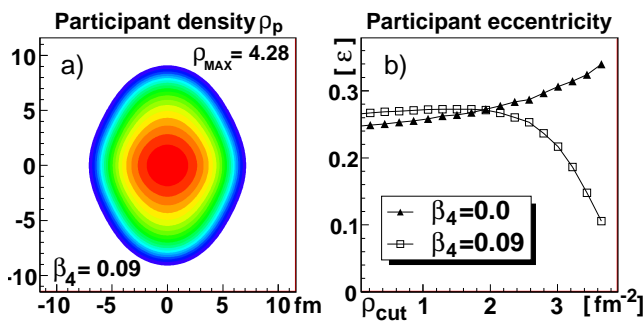


FIG. 1: (Color online) Transverse participant density (a) obtained from optical Glauber model for body-body U+U collisions using  $\beta_2=0.28$  and  $\beta_4=0.093$ . Right panel (b) shows participant eccentricity  $\varepsilon$  of high-density core ( $\rho_p > \rho_{\text{cut}}$ ) for  $\beta_2=0.28$  and  $\beta_4=0$  (as used in [21]) and for  $\beta_4=0.093$ .

$\phi_1, \phi_2$  (z-axis in the beam direction). Optical Glauber model [13] has been used first to clarify the influence of deformation on average eccentricity  $\langle \varepsilon \rangle$  and eccentricity fluctuations in Au+Au collisions.

For given orientations of colliding deformed nuclei  $\theta_1, \theta_2, \phi_1, \phi_2$  and every given impact parameter  $b$ , density of participants  $\rho_{\text{part}}(x, y)$  and density of binary nucleon-nucleon collisions  $\rho_{\text{coll}}(x, y)$  have been used to calculate participant-weighted  $\varepsilon_{\text{part}}$  and collisions-weighted  $\varepsilon_{\text{coll}}$  initial eccentricities [22]

$$\varepsilon = \frac{\sqrt{(\sigma_y^2 - \sigma_x^2)^2 + 4\sigma_{xy}^2}}{\sigma_y^2 + \sigma_x^2}, \quad (2)$$

where  $\sigma_x^2 = \langle x^2 \rangle - \langle x \rangle^2$ ,  $\sigma_y^2 = \langle y^2 \rangle - \langle y \rangle^2$  and the cross-term is  $\sigma_{xy}^2 = (\langle x \cdot y \rangle - \langle x \rangle \langle y \rangle)^2$  (here denoting  $\langle f(x, y) \rangle = \int f(x, y) \rho(x, y) dx dy$ ). Initial eccentricity calculated using Eq.(2) is always a positive number, regardless the orientation of the deformed overlap shape relative to the impact parameter. This corresponds to the elliptic flow measured in the participant plane [23].

From total number of participants  $N_{\text{part}}$  and binary collisions  $N_{\text{coll}}$ , rapidity density of secondary charged multiplicity  $dN_{\text{ch}}/d\eta$  can be determined according to two-component model [24] of particle production:

$$\frac{dN_{\text{ch}}}{d\eta} = (1 - X_{\text{hard}}) \cdot n_{pp} \frac{N_{\text{part}}}{2} + X_{\text{hard}} \cdot n_{pp} N_{\text{coll}} \quad (3)$$

where  $X_{\text{hard}}$  denotes fraction of charged multiplicity produced in binary nucleon-nucleon collisions and  $n_{pp}$  is the energy-dependent charged multiplicity measured in proton-proton collisions. Initial entropy density  $\rho_s(x, y)$  in transverse plane was evaluated according to Glauber ansatz [25]

$$\rho_s(x, y) = \kappa_s [\alpha \rho_{\text{part}}(x, y) + (1 - \alpha) \rho_{\text{coll}}(x, y)] \quad (4)$$

We use  $n_{pp}=2.49$ ,  $X_{\text{hard}}=0.13$  and  $\alpha=0.75$  for collision energy  $\sqrt{s_{NN}} = 200\text{GeV}$ . Using parameter  $\kappa_s = 14.45$

brings our entropy density calculations into agreement with results of Heinz and Kuhlman [21].

Transverse entropy density distributions for selected orientations of Au+Au and U+U collisions are shown in Fig.2. According to expectation, central ( $b=0$ ) tip-tip oriented U+U collisions (main axes of nuclear ellipsoid parallel to the beam direction) give the highest density of the interacting nuclear matter. It is also clearly observed that highest entropy densities in Au+Au collisions are obtained in central ( $b=0$  fm) body-body polarized Au+Au collisions (collinear main axes of nuclear ellipsoids are orthogonal to the beam direction). As shown in plot d) in such collisions initial eccentricity is non-zero due to oblate deformation of  $^{197}\text{Au}$  nucleus and maximum entropy density in such collisions is slightly higher compared to body-body U+U central collisions. Selection of such central Au+Au collisions from the experimental sample of events, however, can be a challenging task.

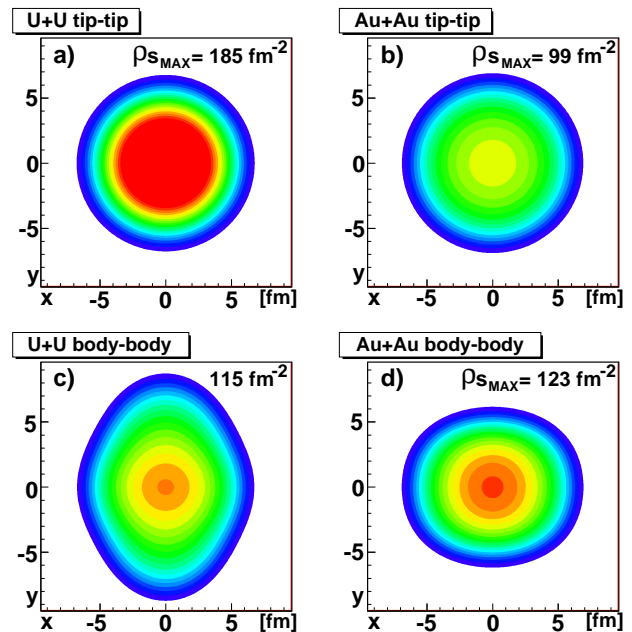


FIG. 2: (Color online) Transverse entropy density for selected orientations in Au+Au and U+U collisions evaluated assuming  $\beta_2 = -0.13$ ,  $\beta_4 = -0.03$  for  $^{197}\text{Au}$  and  $\beta_2 = 0.28$ ,  $\beta_4 = 0.093$  for  $^{238}\text{U}$  at energy  $\sqrt{s_{NN}} = 200$  GeV.

### III. RESULTS AND DISCUSSIONS

**Distribution of participant eccentricity  $\varepsilon_{\text{part}}$  and  $dN_{\text{ch}}/d\eta$  values obtained from optical Glauber simulation [13] for Au+Au collisions assuming oblate  $^{197}\text{Au}$  nuclei (impact parameter  $b < 13.6$  fm increased in 0.1 fm steps) is shown in Fig.3. Nuclear deformation causes variations of eccentricity as well as variations of charged multiplicity  $dN_{\text{ch}}/d\eta$  at given fixed impact parameter  $b$  due to random orientations of deformed nuclei.  $\langle \varepsilon \rangle$  can**

then be calculated as mean value of eccentricities at given interval of multiplicity  $dN_{\text{ch}}/d\eta$  (indicated by solid black circles in Fig.3). For spherical nuclei, single eccentricity  $\varepsilon_{\text{part}}$  and charged multiplicity  $dN_{\text{ch}}/d\eta$  value is obtained for a given impact parameter in the optical Glauber simulation (indicated by solid line in Fig.3). This happens because there are no fluctuations of participant eccentricity from the individual positions of interacting nucleons (at given impact parameter  $b$ ) in the optical Glauber model. Also,  $dN_{\text{ch}}/d\eta$  does not fluctuate at fixed  $b$  in optical Glauber simulation of spherical nuclei collisions. (For spherical nuclei  $\varepsilon \rightarrow 0$  for  $b=0$ .)

It is observed that deformation of colliding nuclei affects eccentricity in the most central collisions since highest multiplicities are obtained for body-body orientations of  $^{197}\text{Au}$  nuclei. In such collisions the eccentricity is enhanced due to non-spherical shape of  $^{197}\text{Au}$  nucleus and consequently average eccentricity  $\langle\varepsilon\rangle$  in very-high-multiplicity Au+Au collisions is increased due to oblate ground-state deformation of  $^{197}\text{Au}$ .

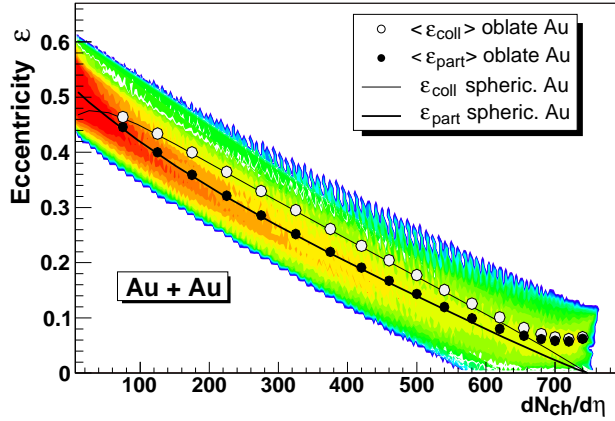


FIG. 3: (Color online) Distribution  $\{\varepsilon_{\text{part}}; dN_{\text{ch}}/d\eta\}$  from optical Glauber simulation for Au+Au ( $\beta_2 = -0.13$ ) collisions at energy  $\sqrt{s_{\text{NN}}} = 200$  GeV. Average participant eccentricity  $\langle\varepsilon_{\text{part}}\rangle$  at given  $dN_{\text{ch}}/d\eta$  is shown as black dots. Solid lines starting at  $dN_{\text{ch}}/d\eta = 740$  represent  $\varepsilon_{\text{part}}$  and  $\varepsilon_{\text{coll}}$  for spherical ( $\beta_2 = 0$ ) Au+Au simulation. Open circles indicate average  $\langle\varepsilon_{\text{coll}}\rangle$  values from  $\{\varepsilon_{\text{coll}}; dN_{\text{ch}}/d\eta\}$  distribution (not shown).

In Monte-Carlo Glauber simulations the eccentricity fluctuations originating from individual positions of interacting nucleons are mixed together with eccentricity fluctuations due to the deformation of nuclei. Width of the fluctuations due to finite number of interacting nucleons  $\sigma_\varepsilon = \sqrt{\langle\varepsilon^2\rangle - \langle\varepsilon\rangle^2}$  and width  $\sigma_\beta$  of fluctuations due to deformation of nuclei add in quadrature and the resulting width of eccentricity fluctuations is:

$$\sigma_\varepsilon = \sqrt{\sigma_\beta^2 + \sigma_\varepsilon^2} \quad (5)$$

In Fig.4 we show charged multiplicity dependence of

average eccentricity  $\langle\varepsilon\rangle$  obtained for deformed Au+Au and U+U collisions. Results obtained assuming  $^{197}\text{Au}$  nucleus to be spherical are also shown. Identical Woods-Saxon density parameters are used in our optical and MC Glauber simulations.

Fluctuations of participant eccentricity due to finite number of interacting nucleons are rather large and it is mainly in central collisions where the influence of ground-state deformation (see Eq.(5)) is visible in Au+Au collisions. For central U+U collisions we observe a cusp in the average eccentricity dependence on charged particle multiplicity  $dN_{\text{ch}}/d\eta$ . This behavior is a consequence of the effective self-orientation of U+U high multiplicity collisions: only U+U collisions with oriented tip-tip configuration contribute to the region of highest multiplicities. In such collisions the initial eccentricity is reduced since transverse profile of longitudinally oriented U nuclei is spherical. The cusp predicted in Fig.4 for the initial eccentricity is a consequence of the binary-collisions-generated contribution to the multiplicity  $dN_{\text{ch}}/d\eta$  in Eq.(3).

This behavior agrees well with results of optical Glauber simulations [26] if the two-component model of particle production [24] is used to calculate  $dN_{\text{ch}}/d\eta$ .

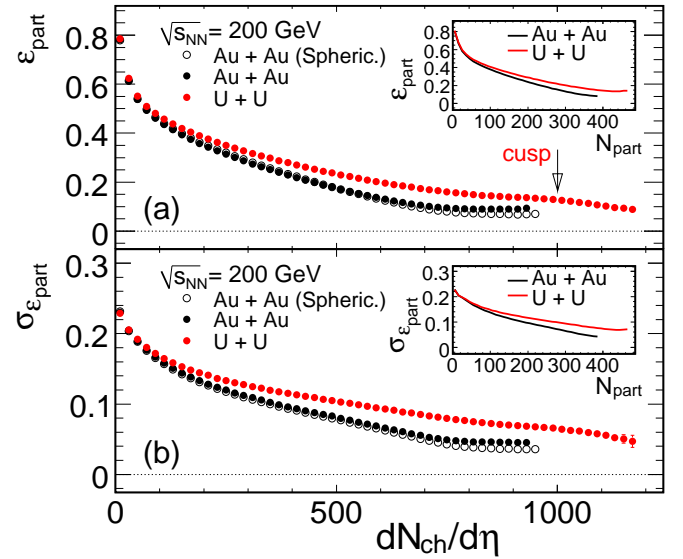


FIG. 4: (Color online) Average eccentricity  $\varepsilon_{\text{part}}$  and width of eccentricity fluctuations  $\sigma_\varepsilon$  as a function of charged particles multiplicity  $dN_{\text{ch}}/d\eta$  within  $|\eta| < 0.5$  obtained from MC Glauber simulation for Au+Au and U+U collisions.

Experimentally, one measures the elliptic flow strength  $v_2$  and elliptic flow fluctuations width  $\sigma_{v_2}$  at given collision centrality characterized by  $dN_{\text{ch}}/d\eta$ . Whether the cusp predicted in Fig.(4) for U+U collisions appears in the elliptic flow dependence on multiplicity  $dN_{\text{ch}}/d\eta$  remains to be verified at RHIC. Assuming hydrodynamical expansion for the compressed QCD matter created in ultra-relativistic collisions of heavy nuclei one can assume  $v_2 = \lambda\langle\varepsilon\rangle$ ,  $\sigma_{v_2} = \lambda\sigma_\varepsilon$  (in paper [20] the factor  $\lambda \approx 0.25$ ), and consequently:  $\sigma_\varepsilon/\langle\varepsilon\rangle \approx \sigma_{v_2}/v_2$ . This allows one to

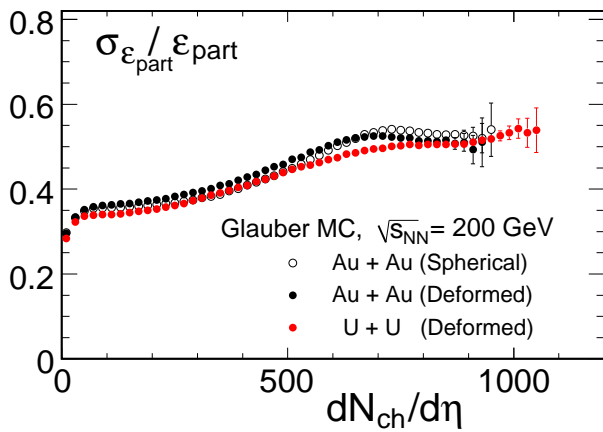


FIG. 5: Ratio  $\sigma_{\epsilon}/\langle\epsilon\rangle$  obtained from MC Glauber simulation for Au+Au and U+U collisions as a function of centrality measured by  $dN_{ch}/d\eta$ .

compare  $\sigma_{\epsilon}/\langle\epsilon\rangle$  value directly with experimentally measured ratio  $\sigma_{v_2}/v_2$ .

One may expect that eventual sudden deviation of experimental value  $\sigma_{v_2}/v_2$  from Glauber-MC evaluated ratio  $\sigma_{\epsilon}/\langle\epsilon\rangle$  studied as a function of particle multiplicity  $dN_{ch}/d\eta$  could be a signal of the phase transition of QCD matter created in relativistic nucleus-nucleus collisions. This might happen due to simultaneous increase of  $\sigma_{\epsilon}$  fluctuations and softening of the equation-of-state of thermalized QCD matter at the phase transition.

Ratio  $\sigma_{\epsilon}/\langle\epsilon\rangle$  for collisions of  $^{197}\text{Au}$  and  $^{238}\text{U}$  nuclei obtained from our MC Glauber simulation is shown in Figure 5. One observes different behaviour for central Au+Au and central U+U collisions. For Au+Au collisions the ratio  $\sigma_{\epsilon}/\langle\epsilon\rangle$  becomes saturated and slightly decreases at  $dN_{ch}/d\eta > 700$ , while in U+U collisions the ratio shows a continuous increase even for high  $dN_{ch}/d\eta$ .

When ratio  $\sigma_{\epsilon}/\langle\epsilon\rangle$  is evaluated (in Glauber Model simulation) as a function of the number of participating nucleons, Au+Au and U+U collisions do not exhibit distinct differences. It is the number of binary nucleon-nucleon interactions  $N_{coll}$  which changes significantly in tip-tip and body-body U+U central ( $b \approx 0$  fm) collisions. Consequently, deformation effects show up in the eccentricity behavior mainly when multiplicity  $dN_{ch}/d\eta$  (see Eq.(3)) is used to quantify the collision centrality.

One observes from Fig.6 that average eccentricity  $\langle\epsilon\rangle$  in Au+Au collisions is influenced significantly in central collisions, if  $^{197}\text{Au}$  oblate deformation is taken into account. The most central bin of Au+Au collisions at RHIC therefore deserves a more detailed study. For example, the average eccentricity  $\epsilon_{part}$  (and measured elliptic flow strength  $v_2$ ) in the highest-multiplicity collisions of oblate  $^{197}\text{Au}$  nuclei (see Fig.4) might show a very small increase at maximal  $dN_{ch}/d\eta$  if the fraction of body-body Au+Au collisions (with

parallel orientations of nuclear ellipsoid axes) is

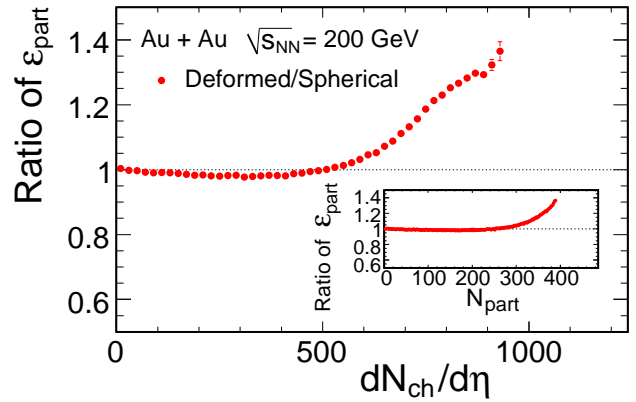


FIG. 6: Ratio of average eccentricities obtained from MC Glauber simulation for Au+Au collisions assuming oblate and spherical ground state of  $^{197}\text{Au}$  nucleus.

effectively enhanced (e.g. by requiring the minimal spectator signals in ZDC calorimeters). However, due to fluctuations of multiplicity  $dN_{ch}/d\eta$  and fluctuating signals of spectators in ZDCs the result of such attempts is not guaranteed.

In non-central collisions ( $dN_{ch}/d\eta < 500$  in Fig.6) we observe only a small decrease of average eccentricity if oblate shape of  $^{197}\text{Au}$  nucleus is assumed. Bulk properties of the partonic matter created at RHIC inferred from the comparison with hydrodynamical calculations of non-central collisions [5] are thus only slightly affected.

To summarize, we have studied the average eccentricity and eccentricity fluctuations in collisions of deformed nuclei using optical and MC Glauber simulations. We observe increased eccentricity fluctuations in collisions of deformed nuclei and increased (up to 30%) average eccentricity for central deformed Au+Au collisions. In central collisions of prolate nuclei we predict a cusp-like behaviour of the average eccentricity if studied as a function of centrality determined by multiplicity  $dN_{ch}/d\eta$ . We think that taking into account nonsphericity of  $^{197}\text{Au}$  nucleus and  $\beta_4$  parameter for  $^{238}\text{U}$  is necessary for the precise understanding of the initial state of the expanding partonic matter created at RHIC. We suggest that from the comparison of experimentally measured ratio ( $\sigma_{v_2}/v_2$ ) and ratio ( $\sigma_{\epsilon}/\langle\epsilon\rangle$ ) obtained in Glauber MC simulations one can obtain information on changes in the behaviour of partonic matter. This can be an additional tool in the search for critical point at RHIC.

Acknowledgements: Authors are indebted to Art Poskanzer for his comments. This work was supported by the U.S. Department of Energy under Contract No. DE-AC03-76SF00098, Slovak Grant Agency for Sciences VEGA under grant No. 2/7116/27, and JINR Dubna.

- 
- [1] J.-Y. Ollitrault, Phys. Rev. D **46**, 229 (1992).  
[2] P.F. Kolb, Phys. Rev. C **68**, 031902(R) (2003).  
[3] J. Adams et al., Nucl. Phys. **A757**, 102 (2005).  
[4] H.-T. Elze and U. Heinz, Phys. Rep. **183**, 81 (1989).  
[5] M. Luzum and P. Romatschke, Phys. Rev. C **78**, 034915 (2008); H.-J. Drescher, A. Dumitru, C. Gombeaud, and J.-Y. Ollitrault, Phys. Rev. C **76** 024905 (2007). D. Teaney, Phys. Rev. C **68**, 034913 (2003).  
[6] M.J. Tannenbaum, Rep. Prog. Phys. **69**, 2005 (2006).  
[7] W. Broniowski, M. Chojnacki, W. Florkowski, and A. Kisiel, Phys. Rev. Lett. **101**, 022301 (2008).  
[8] W. Broniowski and W. Florkowski, Phys. Rev. C **65**, 024905 (2002).  
[9] P. Möller, J.R. Nix, W.D. Myers, and W.J. Swiatecki, At. Data Nucl. Data Tables **59**, 185 (1995).  
[10] T. Abbott et al., Phys. Rev. Lett. **70**, 1393 (1993).  
[11] R. Arnaldi et al., Phys. Rev. Lett. **96**, 162302 (2006).  
[12] G. Wang et al., Nucl. Phys. **A776**, 515 (2008).  
[13] P. Filip, Phys. of Atom. Nuclei, **71**, 1609 (2008).  
[14] B. Hahn, D.G. Ravenhall, and R. Hofstadter, Phys. Rev. **101**, 1131 (1956).  
[15] W.M. Itano, Phys. Rev. **A73**, 022510 (2006).  
[16] C. Nair et al., Phys. Rev. C **78**, 055802 (2008).  
[17] A. Bialas, M. Bleszynski and W. Czyz, Nucl. Phys. **B111**, 461 (1976).  
[18] R.J. Glauber and G. Matthiae, Nucl. Phys. **B21**, 135 (1970); J. Hüfner and J. Knoll, Nucl. Phys. **A290**, 460 (1977).  
[19] K. Hagino, N.W. Lwin, and M. Yamagami, Phys. Rev. C **74**, 017310 (2006).  
[20] P.F. Kolb, J. Sollfrank, and U. Heinz, Phys. Rev. C **62**, 054909 (2000).  
[21] A. Kuhlman and U. Heinz, Phys. Rev. **C72**, 037901 (2005).  
[22] B. Alver, et al., Phys. Rev. Lett. **98**, 242302 (2007).  
[23] J.-Y. Ollitrault, A.M. Poskanzer and S.A. Voloshin, Phys. Rev. **C80**, 014904 (2009).  
[24] D. Kharzeev and M. Nardi, Phys. Lett. **B507**, 121 (2001).  
[25] P.F. Kolb, U. Heinz, P. Huovinen, K.J. Eskola, and K. Tuominen, Nucl. Phys. **A696**, 197 (2001).  
[26] P. Filip, Proceedings of 16-th Conf. of Czech and Slovak Physicists, Hradec Králové 2008; (editor J. Kříž, AS-TRAprint) pp.66-72 (2009); arXiv:0907.4300